

# Measuring Temporal Parameters of Gait with Foot Mounted IMUs in Steady State Running

G. P. Bailey<sup>1</sup>, R. K. Harle<sup>1</sup>

<sup>1</sup>*Computer Laboratory, University of Cambridge, William Gates Building, 15 JJ Thomson Avenue, Cambridge, U.K.  
{gpb29, rkh23}@cl.cam.ac.uk*

## Keywords:

Running, Gait, Temporal Gait Parameters, Foot Kinematics, Continuous Sensing, Toe-Off, Heel-Strike, Cadence, Contact-Time.

## Abstract:

The continuous sensing of running biomechanics provides an opportunity to monitor changes in sporting technique for performance or injury prevention. Inertial sensors are now small enough to integrate into footwear, providing a potential platform for continuous monitoring that does not require additional components to be worn by the athlete and that can be used to assess foot kinematics during running as well as temporal parameters. While temporal parameters of gait are already widely used, they may be combined with the measurement of foot kinematics assessed using a wearable — Inertial Measurement Unit (IMU) based — foot mounted Inertial Navigation System (INS). Assessment of foot pose at times of foot-ground interaction (such as heel-strike and toe-off) is likely to require excellent accuracy in the face of changing technique and speed. We present and evaluate a threshold free algorithm for assessing temporal gait parameters using a foot mounted IMU. We also investigate the impact of errors in temporal gait parameters on the measurement of foot kinematics at these time points. We find that our algorithm has good accuracy, for example we find a mean error  $0.47 \pm 3.84\text{ms}$  for toe-off estimation at a running velocity of  $3.4\text{ms}^{-1}$ . We also find that the magnitude of this error has little affect on some spatial parameter measurements, such as frontal plane foot angle (at a running speed of  $2.3\text{ms}^{-1}$ , mean error at toe-off was  $0.93 \pm 2.07^\circ$ ). However, for others the error in temporal parameters produces larger changes, for example sagittal plane foot angle (at a running speed of  $2.3\text{ms}^{-1}$ , mean error at toe-off was  $4.11^\circ \pm 3.70$ ).

## 1 INTRODUCTION

Biomechanical assessment of movement is a complicated but valuable component of todays elite sports training. Assessment of running gait is particularly important and is usually performed within a laboratory setting. These assessments are often characterised by expensive equipment, manual analysis and subjective metrics. Furthermore the restricted space of a laboratory necessitates evaluation either using a small number of steps or, more often, a treadmill. In neither case is the athlete free to move naturally and there is little guarantee that the gait exhibited is that found in the true sporting arena.

In order to address these issues and to bring such biomechanical assessment to a wider audi-

ence, low-cost inertial sensors are being embedded within consumer products, allowing athletes to be assessed in their natural setting and, additionally, more frequently. Such in-field constant-assessment brings with it additional benefits, including tracking the progress of injury rehabilitation and enabling longitudinal sports science and biomechanical studies

Foot-mounted sensors are popular since lightweight sensors can be embedded within shoes in a convenient, unobtrusive way. They may be able to capture rich data, and have already attracted commercial interest (e.g. the Nike+ shoe). In the future, such sensors may be able to track relevant performance metrics or detect poor or compensatory patterns of gait.

Temporal parameters of gait are of particular

interest when measuring gait. These parameters include the time of heel-strike and toe-off which in turn can be used to assess other temporal parameters, such as flight time, contact time, and cadence, all of which are of interest to athletic coaches and biomechanists.

Temporal parameters of gait give important information regarding the gait cycle, for example contact time (derived from the difference in time between heel-strike and toe-off events) is of use to sprint coaches, where there is a relationship between contact time and speed. Contact time has also been identified as a useful measure of technique during a survey of athlete and coaches perceptions of technology needs (Fleming et al., 2010) and has been suggested as a method of assessing running skill level (Strohrmann et al., 2012). Cadence may also be derived from temporal parameters and is a useful clinical measurement (Dugan and Bhat, 2005). It has been suggested that reduction in stride length may reduce the probability of stress fractures (Edwards et al., 2009), cadence is, therefore, an important metric for coaches and athletes since the only way to reduce stride length — without a change in running velocity — is to increase cadence. Cadence measurement may also be useful for the coach or athlete trying to optimise cadence for performance purposes.

Previous work has enabled the trajectory of the foot to be assessed using foot worn sensors in both running (Bailey and Harle, 2014) and walking (Mariani et al., 2010). Foot trajectory may become even more useful when combined with temporal parameter measurement. The foot trajectory is a rich source of information and it may be helpful to interpret it with the help of temporal gait parameters. The foot makes its contribution to locomotion while in contact with the floor, this means it is important to know the circumstances in which the foot first made contact with the ground, and further, the circumstances with which it terminated contact with the floor.

Providing both temporal parameters and spatial parameters of gait from data obtained from a shoe mounted Inertial Measurement Unit (IMU) is desirable and since spatial parameters have been previously investigated (Bailey and Harle, 2014), assessment of temporal parameters using a foot mounted IMU is an important next step. The purpose of this study is to provide an algorithm to estimate temporal parameters of gait using a foot mounted IMU. The affects of the accuracy of temporal parameters on the estimation of spatial

parameters at heel-strike and toe-off will also be investigated.

We address the following research questions:

- *Is it possible to use a foot mounted IMU to measure temporal parameters of running gait?*

Previous studies have used thresholds with accelerometer data to assess temporal parameters or running gait using a foot mounted IMU. While attempting to use these methods to estimate toe-off we have found them to be inaccurate and unreliable in the face of differing pace. Is it possible to come up with an algorithm that doesn't use thresholds to assess temporal parameters of gait and how accurate is it?

- *How does the accuracy of heel-strike and toe-off estimation affect the measurement of spatial parameters at these time points?*

Previous work has used the strapdown inertial navigation algorithm together with IMUs to recover the trajectory of the foot during each gait cycle in steady state running. Heel-strike and toe-off time could be used in combination with the trajectory of the foot to assess the pose of the foot at these time points. What affect does the error in temporal parameter estimation have on the accuracy of spatial measurements of gait at points in time where the foot interacts with the ground.

## 2 BACKGROUND

Measurement of temporal parameters of gait using wearable sensors for in situ monitoring has been studied in the recent past, however many of the studies available have concentrated on walking gait or investigate temporal parameters with sensors attached to areas of the body that are not the foot and — as previously stated — we believe that placing sensors within the shoe is beneficial in terms of ease and frequency of use. While there has been limited assessment of temporal parameters in running using foot mounted inertial sensors, many other studies have investigated temporal gait parameters either in walking or in running using different sensor placements. Further, different sensor systems have also been used, such as pressure sensors. This section will describe directly related previous work.

A previous work (Strohrmann et al., 2011) investigated the assessment of normalised foot contact time using wearable sensors. To do so the

time of heel-strike and toe-off were estimated using a foot mounted IMU. Placement of the sensor was on the instep of the shoe. Toe-off was detected when the acceleration magnitude exceeded a threshold of  $2g$  following a period where the magnitude of the acceleration was below a particular threshold subsequent to the detected foot strike. No formal evaluation was presented for the accuracy of the recovered toe-off and foot-strike times, but in our experience this algorithm is inaccurate and differing running pace produced significantly different results.

Shank mounted gyroscopes have also been used to assess contact times in running and walking (McGrath et al., 2012) where a gyroscope based algorithm (Greene et al., 2010) was used to determine heel-strike and toe-off times. This was evaluated using optical motion capture data with two different algorithms (Zeni et al., 2008; Hreljac and Marshall, 2000) applied, these algorithms present a limitation to this study as they have been found to be inaccurate in running (Maiwald et al., 2009). The results showed poor to moderate agreement for stance and swing times but performed better for stride times.

While not based on inertial sensors, a number of studies have used pressure sensors embedded within shoes to assess temporal gait parameters. For example, pressure sensors embedded within sprinters shoes have been used to provide contact times (Harle et al., 2011). While the system achieved results with a similar accuracy to force plate data, pressure sensors can be prone to break due to the wiring required and the forces placed upon those wires (and to the sensors themselves) during vigorous motion. For that reason, we have chosen to target the use of IMUs instead of pressure sensors due to the aims of enabling in situ monitoring, potentially over a long period of time. By using an IMU based approach we avoid overcoming the problems with reliability of pressure sensors and make the system viable for lay users and potential manufacturers alike.

## 2.1 Current Methods of Assessing Temporal Parameters

Current methods of assessing temporal parameters are commonly lab based. The ‘gold standard’ method of temporal parameter assessment is the use of force plates. Force plates provide a force/time series, in order to derive temporal parameters a threshold is applied to the vertical component of the measured force — this is

called the Ground Reaction Force (GRF) — to detect the increase in force applied to the plate that corresponds to the contact phase of gait. This threshold is typically set so that it is large enough to be above the noise floor of the sensor and small enough that there is minimal error in the timing, in particular 10N is the typical threshold value (Hreljac and Marshall, 2000; O’Connor et al., 2007; Maiwald et al., 2009). The use of force plates for temporal gait analysis methods has limitations however, and these depend on how the force-plate is used. There are two different scenarios in which the force plate is used, the first is embedded into the floor of the laboratory or running track and the second is embedded within a treadmill.

When embedded into the floor or a running track the area covered by a single force plate is limited to a small area, typically only big enough to assess a single step at a time. This means that the subject being assessed may modify their gait to hit the plate — through adaptations of step length (Abendroth-Smith, 1996) and by extension either contact time or cadence — or miss the area altogether. This means that collecting data on a large number of steps is a laborious task as many trials have to be discarded if the subject modifies their gait or misses the plate and the discarding of steps is subject to human judgement and may be prone to error or bias. Furthermore, there may be some instances where the sequence of steps leading up to a particular manoeuvre, such as cutting, is of importance. This can be very difficult to assess with force plates and so video may be used introducing a laborious and subjective digitisation task. Multiple force plates may be embedded in the track/running surface but the subject being assessed may not hit each one, and the extra instrumentation is a large and unwanted additional cost.

These limitations can to some extent be mitigated by using a treadmill with an embedded force plate, this is the other typical usage scenario. However, this introduces new compromises. Firstly, gait exhibited on a treadmill may be different to that of walking or running over ground, particularly if the subject is unfamiliar with using a treadmill. Secondly, the mechanical nature of the treadmill introduces noise to the force-plate data meaning that the threshold used to find contact times must be increased accordingly, previous studies have used a threshold of 20N (for example (Zeni et al., 2008)). This affects accuracy and consistency with studies based

on overground running, the higher threshold may lead to later estimates of heel-strike and earlier estimates of toe-off when compared to overground force-plate data. Also, more ambitious studies looking at a series of contact times prior to a manoeuvre (such as cutting) are impossible on a treadmill. Finally, they are expensive and relatively uncommon.

The limitations of the above two scenarios suggest a need to be able to assess temporal parameters in-situ but with the ability to assess each step in sequence.

### 3 SENSOR PLATFORM AND DATA CAPTURE

#### 3.1 Inertial Sensors

Capture of inertial sensor data was facilitated using the ION (Imperceptible On-body Node) sensor platform (Harle et al., 2011) with the addition of an IMU providing a three-axis  $\pm 16g$  accelerometer and  $\pm 2000^\circ\text{s}^{-1}$  gyroscope (MPU-6000, InvenSense Inc.) and containing an internal 16 bit Analog-Digital Converter (ADC). The sensor platform is lightweight, weighing approximately 15 grams in total, including battery.

All IMU signals were sampled at 1kHz and logged to on-board flash memory. In all experiments the ION sensor was placed on the lateral side of the shoe in line with the ankle, as seen in Figure 1. The sensor was firmly taped to the outside of the shoe to simulate the scenario where it was built into the shoe, perhaps embedded in the sole in a similar manner to the Nike+ shoe. Since the algorithm presented in this paper is intended for use along side an Inertial Navigation System (INS) the placement on the side of the ankle is informed from an investigation into the validity of the zero-velocity assumption (Foxlin, 2005). It has been shown that the sensor position we have used is among the best suited to using this assumption during a study of foot mounted inertial navigation techniques, including an investigation of different mounting locations on the foot (Pezzetti et al., 2011).

#### 3.2 Ground Truth

Ground truth is important for assessing the ability of any system to assess temporal parameters of gait. However, the gold standard ground truth

of a force plate was unavailable due to a lack of equipment. Access to an optical motion capture system (Vicon) was available however. Previous studies have attempted to validate algorithms based on kinematic data from motion capture to facilitate temporal parameter estimation, these studies have typically focused on walking gait. In order to validate kinematic data based temporal parameter estimation in running a previous study (Maiwald et al., 2009) selected several potential algorithms to evaluate in a running context including their own ‘Foot Contact Algorithm’ (FCA). The evaluation of kinematic data based algorithms for temporal parameters proceeded with comparison to ground reaction force data. They found that previously used algorithms had problems with accuracy but their FCA algorithm was reported to be accurate in both measurement of heel-strike and toe-off with a similar accuracy and precision to the ground reaction force derived measurement. Therefore, we implemented this algorithm to use as ground truth for evaluating our IMU algorithm.

Kinematic data was captured using an optical motion capture system (Vicon Motion Systems, UK) sampling at 240Hz. A treadmill was used in order to capture many steps in a limited motion capture area. The treadmill was set up without any inclination as measured with a spirit level. The ION sensor was attached to a custom jig containing 3 retro-reflective markers (Fig. 1) for the motion capture system, this setup was previously used to evaluate trajectory recovery using a foot-mounted IMU (Bailey and Harle, 2014). The jig in this instance facilitates estimation of the pose of the foot, and the data is used in order to assess the affect of errors in temporal parameters on the estimation of associated spatial parameters. We use the motion capture data when measuring the affect of temporal parameter error on spatial parameter determination to isolate the error cause by the temporal parameters from the potential errors incurred using an INS solution.

The jig adds an additional 30 grams of weight to the system (45 grams total, including ION) but remains comfortable for test runs. The jig was laser cut and the MPU-6000 and retro-reflective markers were aligned with laser-etched outlines to ensure alignment between the jig and the inertial sensor axes. An additional marker was placed on the toe to facilitate using the FCA algorithm. The posterior marker on the jig was used as the heel marker for the FCA algorithm.



Figure 1: Shoe with IMU and Jig for facilitating ground truth capture using the Vicon Motion capture system.

### 3.3 Data Collection

In order to evaluate the temporal parameter estimation algorithm presented in this paper data were collected from 5 participants. Each participant ran for 90 seconds at 4 different speeds. After detection of the running period, 90 steps were extracted for each participant at each speed to ensure the same number of steps were used for each participant. After selecting these 90 steps the heel-strike and toe-off detection was performed for each step. This produced a total of 1800 steps for analysis.

## 4 Temporal Parameter Algorithm

The algorithm proposed in this section takes a divide and conquer approach to finding temporal parameters. Data files are first segmented to find periods of running (run detection), followed by identifying regions that contain a single step from heel-strike to toe-off (step segmentation). Once regions containing heel-strike and toe-off events from a single step are identified, consistent features of the step are used to segment the signal further to get more accurate temporal parameter estimations.

### 4.1 Running Detection and Step Segmentation

This section will describe the process of run detection and step segmentation before returning to the temporal parameter estimation later.

#### 4.1.1 Normalised Auto-correlation based Step Counting

A modified version of the *Normalised Auto-correlation based Step Counting* algorithm (NASC (Rai et al., 2012)) is used to first detect periods of running and then to roughly segment

the signal into individual steps for further inspection to find temporal parameters.

The NASC algorithm exploits the periodicity of gait in order to detect periods of walking. The algorithm uses auto-correlation of an inertial signal. Given that inertial signals measured during gait are periodic the auto-correlation value should be at it's largest at the correct periodicity of the gait cycle. The NASC algorithm was developed to work with inertial sensors placed in any location on the body to detect walking via detecting periodic motion. In this case, the location of the sensor is known and the mode of gait is running rather than walking. This means that the algorithm is modified accordingly to take advantage of this knowledge.

The original algorithm uses the acceleration signal for walk detection. For this work, sagittal plane angular rate ( $g_z$ ) is used since there is lower noise and higher step to step repeatability with this signal for our particular application using a foot-mounted IMU. This can be seen in Figure 2.

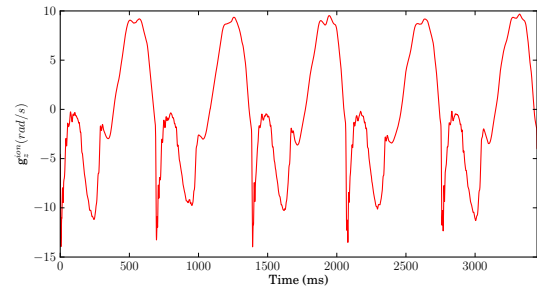


Figure 2: Example showing five steps of sagittal plane angular rate ( $g_z^{ion}$ ).

Given a signal — in this case  $g_z^{ion}(n)$  — the NASC algorithm computes the normalised auto-correlation  $\chi$  for lag  $\tau$  at the  $m^{th}$  sample as described by the following two equations that have been split for readability.

$$\chi(m, \tau) = \frac{\sum_{k=0}^{k=\tau-1} [\alpha(m, \tau, k) \alpha(m + \tau, \tau, k)]}{\tau \sigma(m, \tau) \sigma(m + \tau, \tau)} \quad (1)$$

$$\alpha(i, \tau, k) = g_z^{ion}(i + k) - \mu(i, \tau) \quad (2)$$

In Equations 1 and 2,  $\mu(k, \tau)$  and  $\sigma(k, \tau)$  are the mean and standard deviation of the sequence of samples  $\langle g_z^{ion}(k), g_z^{ion}(k + 1), \dots, g_z^{ion}(k + \tau - 1) \rangle$ .

When the subject wearing the sensor is running (or walking) and  $\tau$  is exactly equal to the period of the acceleration pattern, the normalised auto-correlation will be close to one. However,  $\tau$

is unknown and so NASC tries values of  $\tau$  between selected values of  $\tau_{min}$  and  $\tau_{max}$  to find the value of  $\tau$  for which  $\chi(m, \tau)$  becomes maximum ( $\tau_{opt}$ ). This is described by the following equation.

$$\psi(m) = \max_{\tau=\tau_{min}}^{\tau=\tau_{max}} (\chi(m, \tau)) \quad (3)$$

The implementation presented in (Rai et al., 2012) used a search window ( $\tau_{min}, \tau_{max}$ ) of (0.8s, 2s) for walking, this is based on the typical two step duration of walking. However our scenario is treadmill running and so a search window of (0.6s, 0.9s) is used based on the cadence of the runners tested during the experiments in this paper.

The maximum normalised auto-correlation,  $\psi(m)$ , simultaneously provides two pieces of information (Rai et al., 2012). Firstly, a high value (close to 1) suggests that the person is running or walking since it implies a high level of repeatability in the signal in typical gait cadence ranges, this can be used for run (or walk) detection,. Secondly, the corresponding value of  $\tau = \tau_{opt}$  gives the periodicity of the persons gait. A moving average filter with a 5 second window is used for both  $\psi(m)$  and  $\tau_{opt}$  signals and an example of the resulting signals is given in Figure 3.

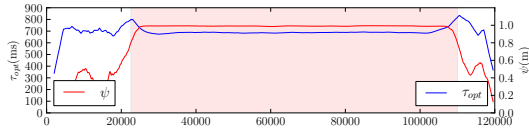


Figure 3: Graph showing  $\tau_{opt}$  and  $\psi(m)$  with 5s moving average filter applied. Shaded area shows the period of detected running.

#### 4.1.2 Run Detection

Periods of running are detected in a similar manner to (Rai et al., 2012). However, since the experiments here are constrained to small data files where we know that running forms the majority of the file, a simpler algorithm is used that doesn't take account of previous states and only uses a threshold on the value of  $\psi(m)$ . A threshold value of 0.8 is used, any value of  $\psi(m)$  above 0.8 is deemed to be a period of running (Figure 3). This detection method would likely need to take into account previous states as in (Rai et al., 2012) were the file to consist of more free form motion with periods of running interspersed with other activities. This was outside of the scope of the current work.

#### 4.1.3 Single Step Segmentation

The NASC algorithm was originally designed for step counting (Rai et al., 2012), however, we are interested in segmenting the steps rather than counting them and therefore the algorithm was modified for this work in order to segment steps. An additional requirement is that it needs to be robust to changes in speed and therefore should not rely on thresholds.

Setting thresholds is not desirable as they are not robust to changes in running technique, running velocity and other factors that affect the magnitude of the peaks of the inertial measurements. This makes robust algorithms that yield few false positives hard to code. This also removes the need for constraints — such as detection of improbable cadences — that are required in order to detect missed peaks due to them being lower than the threshold used.

The NASC algorithm not only enables robust detection of running steps, but the value of  $t_{opt}(m)$  gives an estimate of the time between heel-strike events, this could otherwise be described as the gait period (or the inverse of cadence). This information can be used in order to segment steps based on some repeatable and easily detectable signal feature.

The segmentation proceeds by first looking for one of the clear peaks in the  $g_z^{ion}$  signal near to  $t_{start}$ , the start time of the detected period of running. In order to avoid thresholds we look for the maximum value of  $g_z^{ion}$  in the first two seconds.

$$ts(1) = \text{time}(\max_{t=t_{start}}^{t=t_{start}+2\tau_{opt}(t_{start})} (g_z^{ion}(t))) \quad (4)$$

Here,  $ts(1)$  is the time of the first step segment. This may end up missing a single step at the start, this is due to the size of the initial search window. This window contains approximately two steps worth of data either of which could contain the maximum value so the first is not necessarily selected. This gives a clear and simple to implement method of gaining a single peak to identify as a start point for further segmentation. The peak detected represents the start of the first step segment. The time of subsequent segments are found using in a similar manner by looking in a window defined by the periodicity of the run at the last peak  $\tau_{opt}(ts(n))$ , where  $n$  is the segment number.

$$ts(n+1) = \text{time}(\max_{t=ts(n)+\frac{\tau_{opt}(ts(n))}{2}}^{t=ts(n)+\frac{6\tau_{opt}(ts(n))}{5}} (g_z^{ion}(t))) \quad (5)$$

This results in rough segmentation from which the temporal parameters can be further refined. Figure 4 shows an example of the results of segmentation. Each segment  $(ts(n), ts(n + 1))$  is guaranteed to contain a heel-strike and toe-off event, this is because the maximum sagittal plane angular rate of the foot is during the flight phase of gait. This makes identifying these events a much simpler task than attempting to identify correctly all heel-strike events given a period of data containing multiple steps.

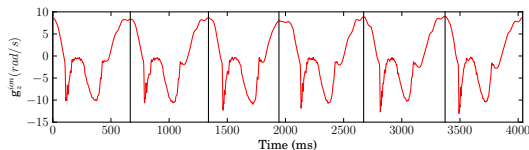


Figure 4: Segmentation of  $g_z^{ion}$  using NASC algorithm to find successive peaks, vertical lines show start times of successive segments  $(ts(n))$ .

## 4.2 Finding Heel-Strike and Toe-Off Points

Now that the running file has been segmented into sections each containing a single heel-strike and toe-off event, the algorithm further splits the step into easy to find pieces before attempting to find the more subtle features associated with heel-strike and toe-off events. The process for each event will be described in the following sections.

### 4.2.1 Heel-Strike

Heel-strike is found by looking for the large changes in signal associated with heel-strike. We again use the  $g_z^{ion}$  signal for this task due to it having relatively little noise compared with the accelerometer signal.

Large changes in a signal can be more easily detected by assessing the first differential. Heel-strike is assessed by inspecting the signal in a region defined using the coarse segmentation defined in Section 4.1.3, sagittal plane angular rate for a subset of a region  $(ts(n), ts(n + 1))$  is shown in Figure 5. For each coarse segment, the differential of the  $g_z^{ion}$  signal is calculated. Then the minimum value of the resulting signal is found, this is shown as the marked circle in Figure 5 and defined in Equation 6.

$$t_{hs}(n) = \text{time}(\min_{t=ts(n)}^{t=ts(n+1)}(g_z^{ion}(t))) \quad (6)$$

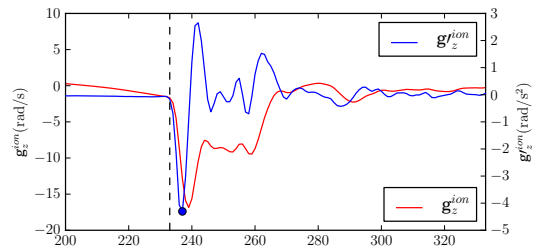


Figure 5: Heel-strike detection from sagittal plane angular rate.

Here  $t_{hs}(n)$  is the first estimate of the time of heel strike for step  $n$ ,  $ts(n)$  is the time of the start of a coarse segment for step  $n$  and  $g_z^{ion}(t)$  is the differential of the  $g_z^{ion}(t)$  signal. This detects a rough estimate for the time of heel-strike which is then refined in the following way.

The peak in the differential represents the maximum rate of change, but this is logically after the heel-strike due to the deformity of the mid-sole of the shoe on impact meaning that the true time of heel-strike should be at the base of this peak. Therefore this estimate is refined by seeking backwards in time to find the base of the local minima. Therefore the algorithm seeks backwards from  $t_{hs}(n)$  up to the point where  $g_z^{ion}(t)$  is greater than  $-0.5$ , this point is then taken to be the detected heel-strike event  $t_{hs}(n)$ . The detected time of heel-strike is shown as the vertical dashed line in Figure 5.

### 4.2.2 Toe-off

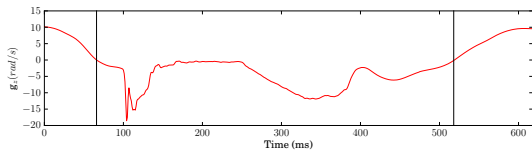
While heel-strike has associated large peaks in inertial data that are easy to detect, the way the foot peels away from the floor before toe-off means that large signal changes don't exist at toe-off using a heel mounted IMU. The best algorithm found by us for toe-off with a heel-mounted sensor depends on finding a small local maxima, in the  $a_y^{ion}(t)$  signal. The  $a_y^{ion}(t)$  channel is aligned with the shank during static standing. As this local maxima is relatively small it is hard to find a reliable algorithm to detect it without further segmentation of the step. Further segmentation of the step allows easier detection of the relevant local maxima.

The segmentation is done by finding the zero crossing in the  $g_z^{ion}(t)$  signal as shown by the vertical lines in Figure 6a. Once the zero crossings are found we look in a window defined using the following formulae.

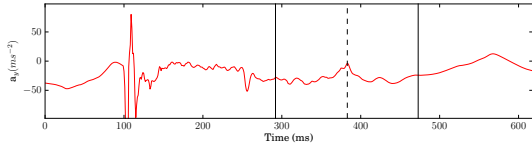
$$w_{start} = c_0 + \frac{(c_1 + c_0)}{2} \quad (7)$$

$$w_{end} = \frac{4(c_1 - w_{start})}{5} + w_{start} \quad (8)$$

Here,  $w_{start}$  and  $w_{end}$  are the times of the start and end of the window respectively and  $c_0$  and  $c_1$  are the first and second zero crossings. This window is marked by the vertical lines in Figure 6b. This narrows down the signal enough that we can now reliably find the minima in the  $a_y^{ion}(t)$  signal between  $w_{start}$  and  $w_{end}$ , this point corresponds to toe-off (Figure 6b).



(a) Further segmentation using zero crossings is demonstrated by the vertical lines.



(b) Toe-off detection. Solid vertical lines show  $w_{start}$  and  $w_{end}$ , dashed vertical line shows detected toe-off.

Figure 6: Further segmentation in order to find toe-off.

This point is less well defined at slower speeds however and may impact upon the accuracy at slower speeds, this is shown in the results of the evaluation.

### 4.3 Applicability

We have chosen the above algorithm after trying many other potential algorithms. This algorithm has the disadvantage that it is most likely dependant on sensor position, particularly alignment, however the alignment chosen for the the sensor and shoe should be easy to replicate with the sensor built into the shoe as it is positioned roughly perpendicular to the surfaces of the midsole. It should also be possible to make small changes to the algorithm for differing alignment such as swapped axes directions meaning finding minimum points need to be substituted for maximum points, for example. This should mean the algorithm remains applicable to a sensor system

built into the shoe, but may not be sufficiently general for an inertial system attached, for example, to the laces of a standard shoe.

### 4.4 Evaluation

The errors in heel-strike and toe-off estimation using the inertial sensor based algorithm in this section are presented in Table 1. The results show mixed accuracy between different running speeds and are dependant on the temporal parameter being assessed. At lower speeds there is slightly lower accuracy and higher variability in the toe-off metric, this is due to the peak in  $a_y^{ion}$  used to assess toe-off being wider and not as sharp leading to less precise estimates at lower speeds. The heel-strike assessment is not subject to this problem due to the relatively large peaks associated with heel-strike.

Table 1: Mean and Standard Deviation of Errors estimating temporal parameters in comparison to those derived from the FCA algorithm. TO = Toe-Off, HS = Heel-Strike

Speed	Error TO (ms)	Error HS (ms)
$2.3\text{ms}^{-1}$	$12.63 \pm 9.90$	$9.86 \pm 6.99$
$2.7\text{ms}^{-1}$	$6.95 \pm 7.74$	$9.91 \pm 4.61$
$3.0\text{ms}^{-1}$	$2.48 \pm 5.99$	$9.82 \pm 3.98$
$3.4\text{ms}^{-1}$	$0.47 \pm 3.84$	$9.89 \pm 3.37$

Contact times were derived from the results of the inertial algorithm for comparison with previous methods demonstrated earlier in this chapter. A small bias of  $-4.37\text{ms}$  was found with limits of agreement  $-23.50\text{ms}$  to  $14.76\text{ms}$ . A Bland-Altman plot can be seen in Figure 7. Cadence was also calculated and a Bland-Altman plot of the results can be seen in Figure 8, there is a small bias of  $0.002$  steps per minute and limits of agreement of  $2.45$  to  $-2.49$  steps per minute, however the figure demonstrates that occasionally there are significant outliers.

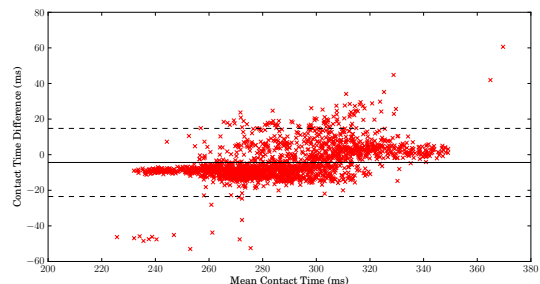


Figure 7: Bland-Altman plot of contact times derived from a heel mounted IMU.

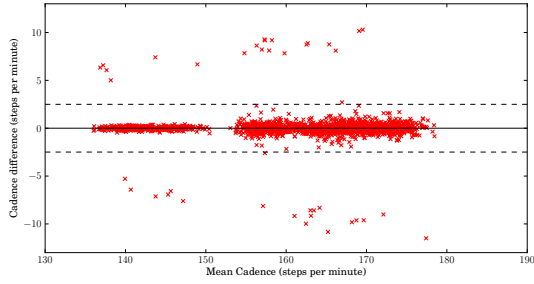


Figure 8: Bland-Altman plot of cadence derived from a heel mounted IMU.

## 5 Affect of Temporal Parameter Estimation Errors on Spatial Parameter Measurement

An algorithm for determining heel-strike and toe-off times using a heel mounted IMU has been presented and evaluated. One of the reasons for developing such an algorithm is to be able to evaluate spatial parameters of gait using foot mounted INS methods (Bailey and Harle, 2014). The temporal parameter estimation described in the previous section is not perfect and has some associated error. This section investigates how that error affects the estimation of spatial parameters of gait at heel-strike and toe-off events.

### 5.1 Evaluation Method

The FCA algorithm provided heel-strike and toe-off times and the jig data were used to derive the angle of the foot at these time points. The angle of the foot is used as a potentially interesting spatial parameter that might be evaluated at toe-off and heel-strike but any other metric could potentially be calculated. At heel-strike the angles of the foot in the sagittal plane ( $\theta_s(t)$ ) and frontal plane  $\theta_f(t)$  were evaluated for each step  $i$  from the Vicon data. These angles were also evaluated at toe-off.

Further, the angle of the foot was recorded for each step at multiple time points, calculated as offsets from the output of the FCA algorithm. For example, for step  $i$ ,  $\theta_s(t)$  would be calculated for a sequence of times  $t = \langle t_{hs}(i) - 20, t_{hs}(i) - 10, t_{hs}(i) + 0, t_{hs}(i) + 10, t_{hs}(i) + 20 \rangle$  (times measured in milliseconds). This series of measurements are designed to show the progression of foot angle (an example of a spatial parameter) in the time period around the temporal event of interest in order to assess accuracy requirements for temporal parameters. Finally, foot orienta-

tion differences are measured between time points measured using the output of the ION based temporal parameter estimation and FCA measured time points.

## 5.2 Results

The angles calculated from the Vicon data at various time points are then turned into deltas from the angle at  $t = t_{hs}(i)$ , for example  $\theta_s(t_{hs}(i) - 20) - \theta_s(t_{hs}(i))$ . The results are shown in Table 2. The results show that the error depends on the measurement being taken, for example the error in the frontal plane at toe off is relatively unchanged 20ms prior to and 20ms after toe-off but the sagittal plane angle varies greatly. This indicates that the spatial parameter being measured may greatly affect the measurement accuracy of temporal parameters required for accurate spatial parameter measurement.

Table 2: Foot angle error at particular time offsets.

Measurement	Error (degrees)
$\theta_f(t_{hs}^{fca}(i) - 20) - \theta_f(t_{hs}^{fca}(i))$	$0.87 \pm 1.43$
$\theta_f(t_{hs}^{fca}(i) - 10) - \theta_f(t_{hs}^{fca}(i))$	$0.58 \pm 1.07$
$\theta_f(t_{hs}^{fca}(i) + 10) - \theta_f(t_{hs}^{fca}(i))$	$2.96 \pm 2.15$
$\theta_f(t_{hs}^{fca}(i) + 20) - \theta_f(t_{hs}^{fca}(i))$	$5.11 \pm 2.95$
$\theta_s(t_{hs}^{fca}(i) - 20) - \theta_s(t_{hs}^{fca}(i))$	$-6.25 \pm 1.91$
$\theta_s(t_{hs}^{fca}(i) - 10) - \theta_s(t_{hs}^{fca}(i))$	$-5.40 \pm 1.38$
$\theta_s(t_{hs}^{fca}(i) + 10) - \theta_s(t_{hs}^{fca}(i))$	$6.77 \pm 1.36$
$\theta_s(t_{hs}^{fca}(i) + 20) - \theta_s(t_{hs}^{fca}(i))$	$12.28 \pm 2.22$
$\theta_f(t_{to}^{fca}(i) - 20) - \theta_f(t_{to}^{fca}(i))$	$1.72 \pm 1.67$
$\theta_f(t_{to}^{fca}(i) - 10) - \theta_f(t_{to}^{fca}(i))$	$0.48 \pm 1.06$
$\theta_f(t_{to}^{fca}(i) + 10) - \theta_f(t_{to}^{fca}(i))$	$0.02 \pm 1.37$
$\theta_f(t_{to}^{fca}(i) + 20) - \theta_f(t_{to}^{fca}(i))$	$0.23 \pm 2.93$
$\theta_s(t_{to}^{fca}(i) - 20) - \theta_s(t_{to}^{fca}(i))$	$7.81 \pm 1.77$
$\theta_s(t_{to}^{fca}(i) - 10) - \theta_s(t_{to}^{fca}(i))$	$3.72 \pm 0.92$
$\theta_s(t_{to}^{fca}(i) + 10) - \theta_s(t_{to}^{fca}(i))$	$-2.78 \pm 0.71$
$\theta_s(t_{to}^{fca}(i) + 20) - \theta_s(t_{to}^{fca}(i))$	$-5.04 \pm 1.38$

Figure 9 shows the distribution of errors for foot angles at both toe-off and heel-strike and includes results for all speeds. Errors at heel-strike show similar results to those at toe-off with the sagittal plane being most affected. The mean error in frontal plane angle at heel-strike between heel-strike measured by FCA vs. ION was  $0.56 \pm 1.22$  degrees. By contrast the mean sagittal plane error was  $-5.56 \pm 2.01$  degrees. Again, this shows the magnitude of errors in spatial parameters that are affected by a difference in measured temporal parameters from reality is dependant on the

spatial parameter being measured. Results may also be dependant on individual technique, Figure 9d shows a small secondary peak at 4 degrees while the main peak is centred on 0 degrees. This may mean that measurement error depends on an individual athletes technique as well as the measurement being evaluated.

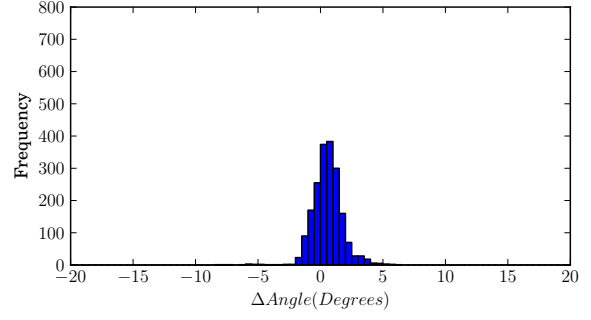
Table 3 shows the angular errors obtained for the time difference between the ION temporal parameters algorithm and the FCA algorithm, broken down by speed. The table shows that the slowest speeds have the largest error for foot angle in the sagittal plane but the frontal plane is again relatively unaffected.

Table 3: Foot angle error between FCA and ION.

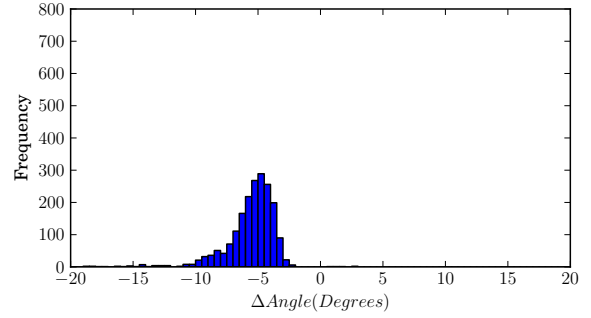
<i>Measurement</i>	<i>Speed</i>	<i>Error (deg)</i>
$\theta_s(t_{hs}^{ion}(i)) - \theta_s(t_{hs}^{fca}(i))$	$2.3\text{ms}^{-1}$	$-4.56 \pm 2.02$
	$2.7\text{ms}^{-1}$	$-5.18 \pm 1.68$
	$3.0\text{ms}^{-1}$	$-5.79 \pm 1.60$
	$3.4\text{ms}^{-1}$	$-6.60 \pm 2.04$
$\theta_f(t_{hs}^{ion}(i)) - \theta_f(t_{hs}^{fca}(i))$	$2.3\text{ms}^{-1}$	$0.33 \pm 1.25$
	$2.7\text{ms}^{-1}$	$0.46 \pm 1.16$
	$3.0\text{ms}^{-1}$	$0.71 \pm 1.25$
	$3.4\text{ms}^{-1}$	$0.71 \pm 1.18$
$\theta_s(t_{to}^{ion}(i)) - \theta_s(t_{to}^{fca}(i))$	$2.3\text{ms}^{-1}$	$4.11 \pm 3.70$
	$2.7\text{ms}^{-1}$	$2.51 \pm 2.82$
	$3.0\text{ms}^{-1}$	$1.06 \pm 2.51$
	$3.4\text{ms}^{-1}$	$0.22 \pm 1.64$
$\theta_f(t_{to}^{ion}(i)) - \theta_f(t_{to}^{fca}(i))$	$2.3\text{ms}^{-1}$	$0.93 \pm 2.07$
	$2.7\text{ms}^{-1}$	$0.08 \pm 1.12$
	$3.0\text{ms}^{-1}$	$0.14 \pm 0.97$
	$3.4\text{ms}^{-1}$	$0.14 \pm 0.52$

## 6 CONCLUSIONS

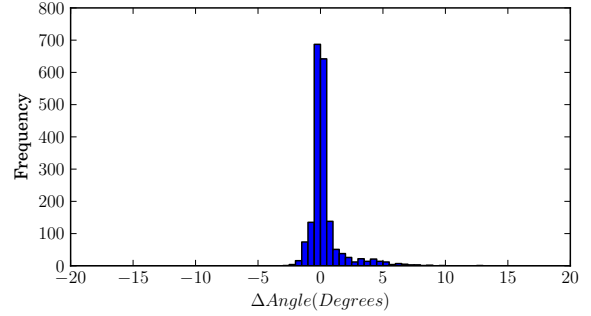
A method of reliably finding temporal parameters of gait from a foot mounted IMU has been presented and evaluated. The method presented is free of thresholds that may be unreliable in the face of changing technique and running pace. However, it is likely that the algorithm will only work with the sensor position used within this paper. The algorithm was designed with a view to the sensors being built into the mid-sole of the shoe so we view this as a minor limitation. The algorithm has usable accuracy for temporal parameter estimation but its accuracy for toe-off is somewhat dependant on running velocity. The impact of the magnitude of this error on the estimation of spatial metrics was also investigated



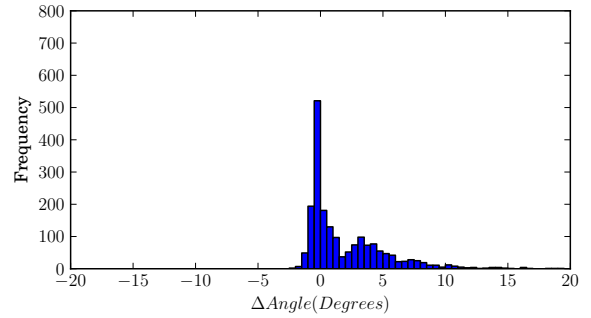
(a)  $\theta_f(t_{hs}^{ion}(i)) - \theta_f(t_{hs}^{fca}(i))$



(b)  $\theta_s(t_{hs}^{ion}(i)) - \theta_s(t_{hs}^{fca}(i))$



(c)  $\theta_f(t_{to}^{ion}(i)) - \theta_f(t_{to}^{fca}(i))$



(d)  $\theta_s(t_{to}^{ion}(i)) - \theta_s(t_{to}^{fca}(i))$

Figure 9: Difference in foot angle at temporal events measured by the ION and FCA algorithms.

and shows that some metrics are likely to be more affected than others. We find that for some metrics there are minimal errors in spatial parameters measured at time points derived from the foot IMU data. Further work should seek to evaluate the temporal parameter algorithm to check for accuracy and robustness in outdoor over ground running to enable practical training and biomechanical assessment tools.

## REFERENCES

- Abendroth-Smith, J. (1996). Stride Adjustments during a Running Approach toward a Force Plate. *Research Quarterly for Exercise and Sport*, 67(1):97–101.
- Bailey, G. and Harle, R. (2014). Assessment of Foot Kinematics During Steady State Running Using a Foot-mounted IMU. *Procedia Engineering*, 72:32–37.
- Dugan, S. A. and Bhat, K. P. (2005). Biomechanics and analysis of running gait.
- Edwards, W. B., Taylor, D., Rudolphi, T. J., Gillette, J. C., and Derrick, T. R. (2009). Effects of stride length and running mileage on a probabilistic stress fracture model. *Medicine and Science in Sports and Exercise*, 41:2177–2184.
- Fleming, P., Young, C., Dixon, S., and Carré, M. (2010). Athlete and coach perceptions of technology needs for evaluating running performance. *Sports Engineering*, 13(1):1–18.
- Foxlin, E. (2005). Pedestrian tracking with shoe-mounted inertial sensors. *IEEE Computer Graphics and Applications*, 25(6):38–46.
- Greene, B. R., McGrath, D., O’Neill, R., O’Donovan, K. J., Burns, A., and Caulfield, B. (2010). An adaptive gyroscope-based algorithm for temporal gait analysis. *Medical and Biological Engineering and Computing*, 48:1251–1260.
- Harle, R., Taherian, S., Pias, M., Coulouris, G., Hopper, A., Cameron, J., Lasenby, J., Kuntze, G., Bezodis, I., Irwin, G., and Kerwin, D. G. (2011). Towards real-time profiling of sprints using wearable pressure sensors. *Computer Communications*.
- Hreljac, A. and Marshall, R. N. (2000). Algorithms to determine event timing during normal walking using kinematic data. *Journal of Biomechanics*, 33:783–786.
- Maiwald, C., Sterzing, T., Mayer, T., and Milani, T. (2009). Detecting foot-to-ground contact from kinematic data in running. *Footwear Science*, 1(2):111–118.
- Mariani, B., Hoskovec, C., Rochat, S., Büla, C., Penders, J., and Aminian, K. (2010). 3D gait assessment in young and elderly subjects using foot-worn inertial sensors. *Journal of Biomechanics*, 43:2999–3006.
- McGrath, D., Greene, B. R., O’Donovan, K. J., and Caulfield, B. (2012). Gyroscope-based assessment of temporal gait parameters during treadmill walking and running. *Sports Engineering*, 15(4):207–213.
- O’Connor, C. M., Thorpe, S. K., O’Malley, M. J., and Vaughan, C. L. (2007). Automatic detection of gait events using kinematic data. *Gait and Posture*, 25:469–474.
- Peruzzi, A., Della Croce, U., and Cereatti, A. (2011). Estimation of stride length in level walking using an inertial measurement unit attached to the foot: A validation of the zero velocity assumption during stance. *Journal of Biomechanics*, 44:1991–1994.
- Rai, A., Chintalapudi, K. K., Padmanabhan, V. N., and Sen, R. (2012). Zee: Zero-Effort Crowdsourcing for Indoor Localization. In *Proceedings of the 18th annual international conference on Mobile computing and networking - Mobicom ’12*, page 293.
- Strohrmann, C., Harms, H., Tröster, G., Hensler, S., and Müller, R. (2011). Out of the lab and into the woods: kinematic analysis in running using wearable sensors. In *Proceedings of the 13th international conference on Ubiquitous computing*, pages 119–122. ACM.
- Strohrmann, C., Rossi, M., Arnrich, B., and Troster, G. (2012). A Data-Driven Approach to Kinematic Analysis in Running Using Wearable Technology. *2012 Ninth International Conference on Wearable and Implantable Body Sensor Networks*, pages 118–123.
- Zeni, J. A., Richards, J. G., and Higginson, J. S. (2008). Two simple methods for determining gait events during treadmill and overground walking using kinematic data. *Gait and Posture*, 27:710–714.